

# QUALITY PREDICTION IN INJECTION MOLDING BASED ON THERMAL IMAGES WITH CONVOLUTIONAL NEURAL NETWORKS

*Dimitri Kvaktun, Yannick Elsinghorst and Reinhard Schiffers, University of Duisburg-Essen, Institute of Product Engineering (ipe), Duisburg, Germany*

## Abstract

Precise predictive models are required for the use of machine learning methods for quality control in injection molding. Thermal images offer the advantage of containing information in the data that is not available in machine and process data. Currently, convolutional neural networks (CNN) have numerous applications in image recognition. Therefore, the objective of this work was to investigate the application of convolutional neural networks to thermal images of injection molded parts. For this purpose, 751 injection molding cycles from a central composite design were used. The goal was to predict the weight, height, and width of the injection molded part. The results were also compared with classical machine learning methods. Depending on the quality parameters, the networks were able to achieve an  $R^2$  of up to 0.91 and were thus among the three best methods.

## Introduction

Injection molding is one of the most common mass production processes, enabling the manufacture of complex geometries at low cost. Therefore, there are various strategies for process optimization and control. Most of them focus on using machine and process data during the cycle to compensate for deviations from target values [1]. In recent years, machine learning approaches have been proposed and applied for quality prediction. Prediction models can therefore predict the quality of parts such as shrinkage, weight, or dimensions [2].

Pressure and temperature sensors are available in the mold to provide information that is used by many control strategies [3]. However, this type of sensor technology has disadvantages such as high cost, space requirements in the mold, and the property of creating marks on the molded parts that may need to be hidden [4]. Instead of in-mold sensors, the use of indirect measurement methods such as thermal imaging cameras is possible [5,6]. Compared to in-mold sensors, they provide more information about the internal properties of the molded part [7].

Therefore, this study answers the following research questions:

- How do different process settings affect thermal images (TI) and quality criteria?

- How good is the prediction performance of convolutional neural networks on TI?
- How does the prediction performance compare to classical machine learning algorithms using machine and process data?

The rest of this paper is organized as follows. First, convolutional neural networks are explained. Then, the experimental setup for data generation is presented. Next, the overall quality prediction framework used for the classical machine learning methods is outlined, followed by a presentation and discussion of the results. Finally, an outlook on further studies is given.

## Convolutional neural networks

Convolutional neural networks (CNN) [8] are a special form of artificial neural networks (ANN) and are currently widely used for image analysis.

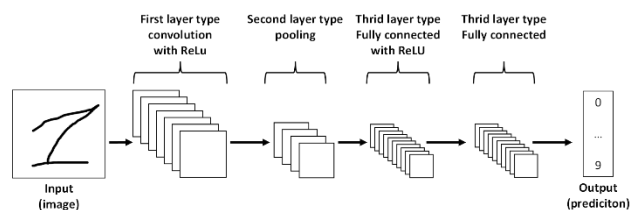


Figure 1. Example for a CNN architecture with four layers [9].

Convolutional neural networks usually consist of three types of layers (see Figure 1), with the number of layers depending on the problem. A simple CNN consists of the following structure: the input to the CNN contains the pixel values of the image. The first layer is a convolutional layer that operates like a filter on the image. The filter consists of a series of numbers and slides through the input pixel values, calculating the scalar product for each value. The application of this step results in a feature map. Through this step, the network learns specific features at a given position from the input images, such as edges or lines, and is later able to recognize objects when new images have the same features as in the feature map. In addition, the feature map is processed by a rectified linear unit (ReLU), which removes all black elements. This reduces the complexity and removes the linearity between colors, making the features of the image more prominent. The second layer is called the pooling layer and reduces the dimensionality of the feature map. In addition, this layer makes the CNN

more robust to object shifts and distortions. The most popular pooling strategy is max pooling, where the maximum value of a section is extracted from the feature map. The last layer is a typical fully connected layer as in a normal ANN. Here, the feature map is converted into a one-dimensional field that is connected to the final output of the network. The training of the CNN consists in finding the features in the convolutional layer and the weights in the fully connected layer that minimize the error between prediction and actual value [9].

## Experimental setup

The experiments were carried out with an all-electric injection molding machine type 120-380 PX with a three-zone screw of 40 mm diameter (KraussMaffei Technologies GmbH, Munich, Germany). The machine is part of a production cell consisting of the injection molding machine, a handling system, a conveyor belt and 100 % inline quality control.

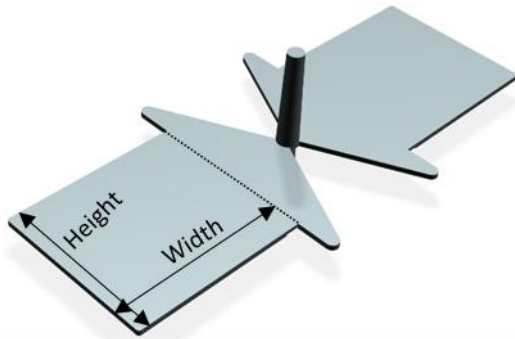


Figure 2. Plate specimen used for data generation.

A symmetrical plate specimen (see Figure 2) was taken for data generation. However, only one half was used for analysis to get the highest possible resolution available of the images. The mold was manufactured by Axxicon Moulds Eindhoven B.V. and is equipped with two Unisens 6157BA cavity pressure sensors (Kistler Instrumente GmbH, Sindelfingen, Germany). The material was a polyamide 6 (Durethan B30S 000000, Lanxess Deutschland GmbH, Cologne, Germany) and was dried to achieve the required residual moisture content.

The weight and dimensions of the specimen were used as quality criteria for prediction by the models. The weight was measured using an Entris 153I-1S balance (Sartorius Lab Instruments GmbH & Co. KG, Göttingen, Germany). The information was read out using Simple Data logger software (Smartlux S.à.r.l., Born, Luxembourg). An Optris PI400i camera (Optris GmbH, Berlin, Germany) with a resolution of 382x288 pixels was used for the TI.

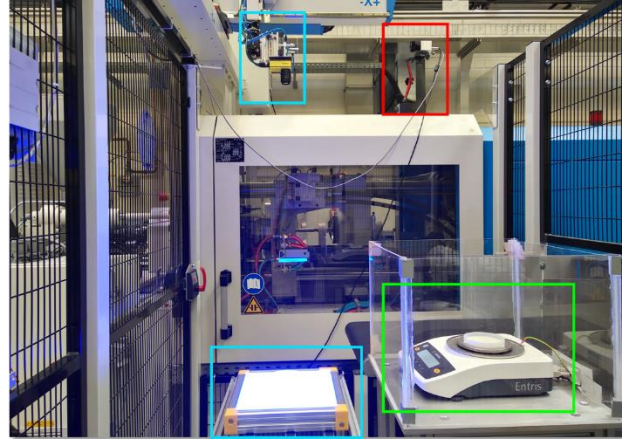


Figure 3. Production cell with thermal camera (red box), balance (green box) and smart camera system (blue box).

The position and overall setup of the production cell can be seen in Figure 3. The position of the thermal camera was chosen outside the machine, because otherwise it was not possible to photograph the molded parts from the front. In addition, a 12 MP In-Sight 9912 smart camera system (Cognex Corporation, Natick, USA) was used to measure the width and height of the part in-line. The camera was equipped with a 50 mm 4/3" lens. The dimensional information was automatically extracted from the monochrome images using Cognex's In-Sight Explorer software. Machine and process parameter were taken from the build-in sensors of the machine. To achieve differences in the TI a central composite design (CCD) was carried out. The following parameters were varied: injection speed, holding pressure time, cooling time, mold temperature and nozzle temperature. Table 1 shows the different factor levels.

Table 1. The CCD with the factor levels.

Factors		Level		
ID	Setting value	-	0	+
A	Injection speed [mm/s]	80	100	120
B	Holding pressure time [s]	4	6	8
C	Cooling time [s]	6	8	10
D	Mold temperature [°C]	70	80	90
E	Nozzle temperature [°C]	255	265	275

A total of 43 design points were performed, with 22 cycles per design point included in the modeling. With intermediate cycles, whose sole purpose was the thermal stabilization of the process, 1096 were recorded. After data preprocessing, however, only 751 cycles could be utilized. Reasons for removing data were incomplete quality records.

## Setup of the CNN

The CNN was implemented in Python using Tensorflow and Keras. Initially, 20% of the data was randomly split for the test data set. 60% of the data was used for training the model and 20% for validation. To improve the training of the CNN, the color values from 0 to 255 were scaled to 0 to 1.

The image input vector had a size of  $382 \times 288 \times 3$ , which was then processed by the following CNN. The network consisted of three convolutional layers, each with a max-pooling layer (size  $2 \times 2$ ; no stride) and the ReLU activation function. A  $3 \times 3$  filter was used in each convolutional layer. The first layer had 16 filters, the second 32, and the last 64. After the convolutional layers, the data were flattened to a  $108288 \times 1$  vector. To avoid overfitting, a dropout of 0.01 was implemented. Next, a fully-connected layer transformed this vector into a  $512 \times 1$  vector, which was then used for quality prediction. The CNN was optimized using the Adadelta-algorithm [10]. This structure was selected through iterative manual testing.

## Quality prediction framework

For the comparison with classical machine learning algorithms, the approach first presented in [11] was used. The machine and process data from the 751 injection molding cycles were divided into 60 % training, 20 % validation, and 20 % testing according to the division for the CNN. For the feature processing step, feature selection was chosen with a reduction of the feature space to the best five features. Here, forward search with correlation-based feature selection and Pearson correlation coefficient was used [12]. The selected machine learning algorithms were multiple linear regression (MLR) [13], support vector machines (SVM) [14], binary decision trees (DT) [15], k-nearest-neighbors (kNN) [16], ensemble methods (EM) (LSBoost [13] & random forest [17]) and Gaussian process regression (GP) [18]. The hyperparameters were optimized using Bayesian optimization [19] and 5-fold cross validation [20]. The coefficient of determination ( $R^2$ ) obtained on the test data set was used to evaluate the algorithms. The system was implemented in Python using the scikit-learn library.

## Results

### Effects of the CCD on the thermal images

To investigate the influence of the parameters on the images, the star points of the CCD are particularly suitable, since here only one parameter was varied compared to the center point. Therefore, Figure 4, which was taken from the center point, is used as a reference.

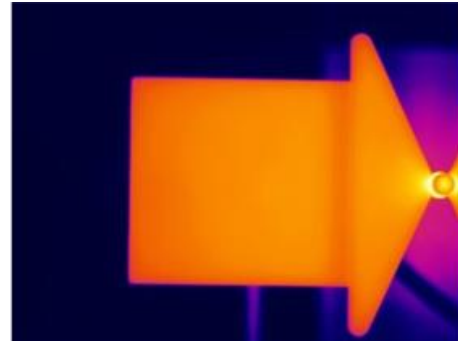


Figure 4. Image taken from the center point of the CCD.

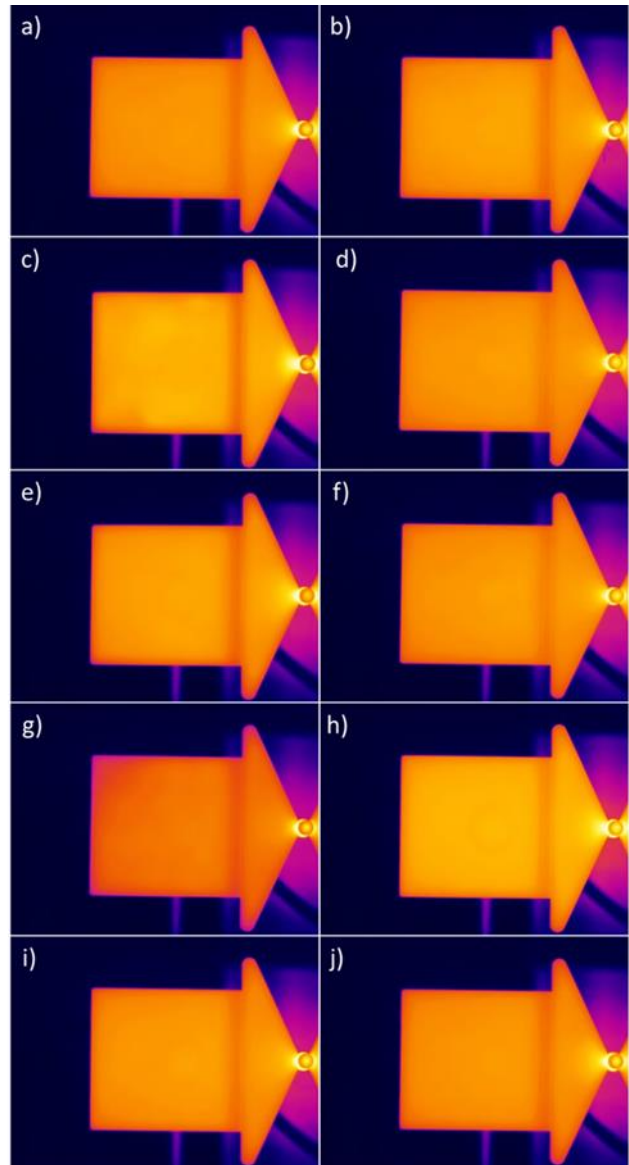


Figure 5. Different TI depending on the varied process parameters of the CCD.

Figures 5a and 5b first show the influence of parameter A, the injection speed. This was 68 mm/s in Figure 5a and

125 mm/s in Figure 5b. Compared to Figure 4, there is no significant difference. Only Figure 5b was slightly brighter than Figure 5a. In 5c (B = 2.8 s) and 5d (B = 9.2 s), the influence of holding pressure time can be seen. The temperature in 5c was lower than in Figure 4 and the overall temperature distribution was more inhomogeneous. Figures 5e and 5f show the influence of the parameter C, the cooling time. In Figure 5e, the time was reduced to 4.8 s, resulting in a warmer part, while in Figure 5f, the time was increased to 11.2 s, resulting in a darker image and thus a cooler part. In Figures 5g and 5h, the mold temperature was varied (D = 64 °C; D = 94 °C). The part in Figure 5g was cooler than in the center and the coolest in all the images of Figure 5, while the part in Figure 5h was lighter than in Figure 4 and the lightest overall. The effects of nozzle temperature can be seen in Figures 5i (E = 249 °C) and 5j (E = 281 °C). The image in Figure 5i was slightly brighter than in Figure 4, although the images at this point in the experiment were very similar to the center point.

### Effects on the part weight

As will be seen later in the model evaluation section, the automatically recorded dimensions provided a poorer data basis, which is why only the weight is referred to in this section. Figure 6 shows the influence of the different parameters varied during the CCD on the part weight. For reasons of readability, a representation with star points has been omitted. Therefore, the weight values of the last three cycles of each design point were taken and averaged. Factor B, holding pressure time, had the greatest influence on part weight. A longer holding pressure time (blue bars) resulted in a higher part weight, while a lower holding pressure time (orange bars) resulted in a lower weight. For mold temperature (factor D), a lower temperature resulted in a higher weight. At design points 2 to 9 and 18 to 25, D- was set, and here the weight averaged 24.85 g and 24.75 g, while at design points with D+ (10 to 17 and 26 to 33) the weight averaged 24.71 g and 24.60 g, respectively. Moreover, in the design points with lower nozzle temperature (factor E, 2 to 17), the weight was higher on average (24.78 g) than in the design points with higher nozzle temperature (18 to 33), which was 24.67 g on average. The influence of injection speed (factor A), which was varied at each design point, and the influence of cooling time (factor C), which was varied at every fourth design point, cannot be identified clearly from the weight values. However, the influence of the injection speed seems to be small, since the weight values after changing the parameter (e.g., at design point 2 & 3 or 4 & 5) have almost the same values.

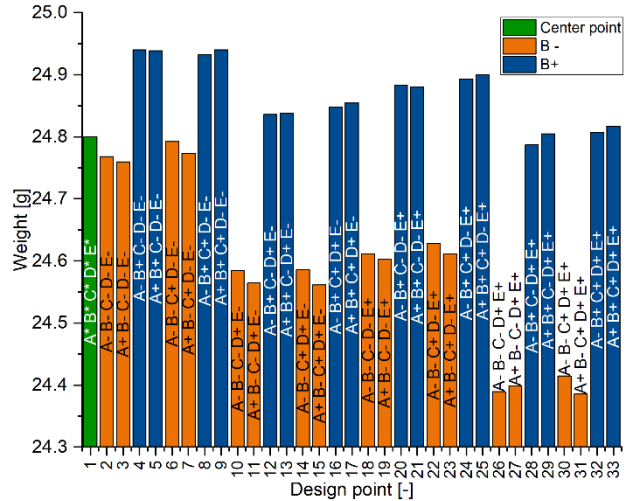


Figure 6. Influence of the individual injection molding parameters on the part weight without star points.

### Prediction performance of the CNN

The main research question was how well CNN can be used on thermal images for quality prediction. The best model after 6000 training iterations (also called epoch) was used for prediction. Figure 7 shows the prediction of CNN for the unknown test data set.

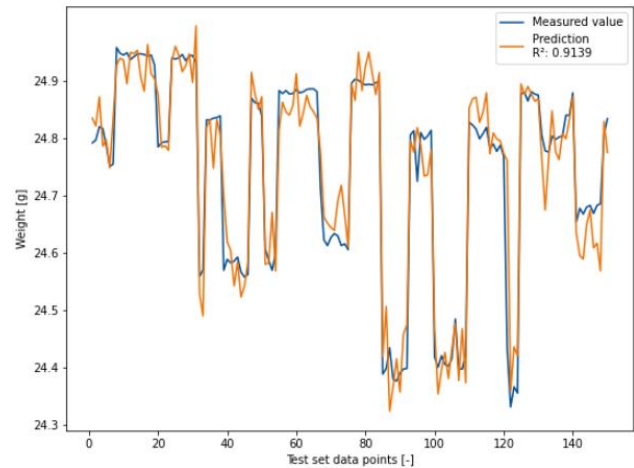


Figure 7. Prediction of part weights using the implemented CNN on the unknown test data set.

The blue curve represents the actual measured values of the part weight, while the orange curve is the prediction of the CNN. The best model was able to achieve an R<sup>2</sup> of 0.9139. The coefficient of determination for the height and width (not shown) of the part was lower at 0.4113 and 0.4714.

## Comparison of prediction performances

The second research question was how well the prediction performance of the CNN compares to more classical machine learning algorithms such as support vector machines, etc. Figure 8 shows the  $R^2$  value for the three quality criteria using the test data sets. For training the other models, the machine and process data recorded in parallel with the TI were used. The  $R^2$  value for the weight data set is generally higher than for the two dimension criteria. The highest  $R^2$  value for weight was achieved by the ensemble model with an  $R^2$  value of 0.94. CNN had the third highest value at 0.91. For height and width, the highest  $R^2$  was obtained by the kNN model with 0.68 and 0.79, respectively. The prediction quality of the CNN for height was the second worst of all the models at 0.41, with only SVM being worse at 0.40. For width, the  $R^2$  of the CNN was 0.47, the worst of all.

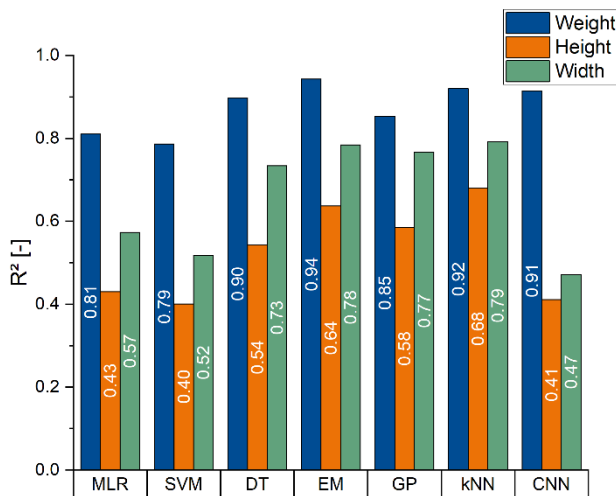


Figure 8.  $R^2$  of different prediction models on the test data sets.

## Discussion

Considering the results, it can be stated that the database was basically suitable for training the machine learning methods. Thus, the expectations regarding the influences of the varied parameters on the TI and the quality variables were met. The effect of parameter A, injection speed, on TI can be explained because the melt is sheared less at lower speeds, which means that the material heats up less. Correspondingly, the opposite is true at high speeds (cf. Figure 5a & 5b). The effect of holding pressure time on the images can be explained by the fact that with a shorter holding pressure time, the cycle time is correspondingly shorter and the part, therefore, cools down less. In addition, a shorter holding pressure time means that less material is injected, which also reduces the weight of the part. The same consideration applies to the change in cooling time and the resulting images. In addition, the

influences of mold and nozzle temperature can be explained by the fact that the temperature level of the demolded part is lower or higher, which can also be seen in the pictures. The influence of the mold temperature on the weight can be interpreted by the fact that the material cools faster at low temperatures and therefore shrinks more, which is why more material can be injected.

In general, it can be said that CNN trained with TI can achieve good prediction performance. The worse  $R^2$  for both dimension predictions indicates that the resolution of the smart camera system was not high enough, which is why all methods performed worse than for the weight data set. However, the CNN seems to be particularly sensitive here. A major disadvantage of CNN is the long training time. The configuration used in this study required 6 hours for training, which is too long compared to the classical methods that required between 10 and 30 minutes.

## Conclusion and outlook

In this study, we investigated the suitability of TI for predicting the quality of injection molded parts. Convolutional neural networks were used for this purpose. The performance was also compared with classical machine learning methods such as support vector machines or gaussian process regression. A total of six other methods was used. A central composite design was performed, using 751 cycles to build the model after preprocessing the data. In general, the CNN was able to achieve a high  $R^2$  of 0.91 for part weight prediction. However, this was only the third highest model quality, the highest being 0.94 by an ensemble model. In addition, the CNN achieved the worst results for the two dimensions with an  $R^2$  of 0.41 for height and 0.47 for width.

In future studies, the training duration of the CNN should be reduced. Since the network architecture was manually selected in this work, the duration can be reduced by optimizing the respective architecture. We also used color images, which increase the dimension of the input. Here, converting to grayscale should speed up the training. To increase the prediction accuracy of the CNN, a higher-resolution camera could be used. This should allow details to be seen even better and thus better relationships to quality features. In addition, instead of an experimental design, a data set should be generated from a stable process. These are more challenging for machine learning methods due to less variation in the quality features, but closer to industrial applications.

## Acknowledgements

We would like to thank the PLEXPART GmbH (Aalen, Germany) for supplying the thermal camera used in the experiments.

## References

1. C. Fernandes, A.J. Pontes, J.C. Viana, A. Gaspar-Cunha, *Modeling and Optimization of the Injection-Molding Process: A Review*, *Adv. Polym. Technol.*, **2**, 37 (2016).
2. O. Ogorodnyk, O.V. Lyngstad, M. Larsen, K. Martinsen, *Prediction of Width and Thickness of Injection Molded Parts Using Machine Learning Methods*, In: Kishita Y, Matsumoto M, Inoue M, Fukushige S, editors. *EcoDesign and sustainability I*. Singapore: Springer, (2021).
3. C. Hopmann, A. Reißmann, J. Heinisch, *Influence on Product Quality by pvT-Optimised Processing in Injection Compression Molding*, *International Polymer Processing Journal of the Polymer Processing Society*, **2**, 31 (2016).
4. T. Ageyeva, S. Horváth, J.G. Kovács, *In-Mold Sensors for Injection Molding: On the Way to Industry 4.0*, *Sensors*, **16**, 19 (2019).
5. P. Nagorny, M. Pillet, E. Pairel, R.L. Goff, L. Jérôme, W. Marlène, P. Kiener, *Quality Prediction in Injection Molding*, *IEEE International Conference on Computational Intelligence and Virtual Environments for Measurement Systems and Applications*, (2017).
6. P. Nagorny, T. Lacombe, H. Favreliere, M. Pillet, E. Pairel, R.L. Goff, M. Wali, J. Loureaux, P. Kiener, *Generative Adversarial Networks for geometric surfaces prediction in injection molding*, *IEEE International Conference on Industrial Technology*, (2018).
7. K. Bula, L. Rozanski, L. Marciniak-Podsadna, D. Wróbel, *The use of IR thermography to show the mold and part temperature evolution in injection molding*, *Archives of Mechanical Technology and Materials*, **1**, 36 (2016).
8. Y. Lecun, L. Bottou, Y. Bengio, P. Haffner, *Gradient-based learning applied to document recognition*, *Proceedings of the IEEE*, **11**, 86 (1998).
9. K.T. O'Shea, R. Nash, *An Introduction to Convolutional Neural Networks*, (2015).
10. M.D. Zeiler, *ADADELTA: An Adaptive Learning Rate Method*, (2012).
11. A. Schulze Struchtrup, D. Kvaktun, R. Schiffers, *A Holistic Approach to Part Quality Prediction in Injection Molding Based on Machine Learning*, *Advances in Polymer Processing 2020: Proceedings of the International Symposium on Plastics Technology*, 1st ed. Berlin, Heidelberg: Springer Berlin Heidelberg, (2020).
12. A. Schulze Struchtrup, D. Kvaktun, R. Schiffers, *Comparison of feature selection methods for machine learning based injection molding quality prediction*, *AIP Conference Proceedings*, 2289(1):20052, (2020).
13. T. Hastie, R. Tibshirani, J.H. Friedman, *The elements of statistical learning: Data mining, inference, and prediction*, 12th ed. New York, NY: Springer, (2017).
14. A.J. Smola, B. Schölkopf, *A tutorial on support vector regression*, *Statistics and Computing*, **3**, 14 (2004).
15. L. Breiman, *Classification and regression trees*, Boca Raton: Chapman & Hall, (1998).
16. G. Biau, L. Devroye, V. Dujmović, A. Krzyżak, *An affine invariant k-nearest neighbor regression estimate*, *Journal of Multivariate Analysis*, 112 (2012).
17. L. Breiman, *Random Forests*. *Machine Learning*, **1**, 45 (2001).
18. C.E. Rasmussen, C.K.I. Williams, *Gaussian processes for machine learning*, 3rd ed. Cambridge, Mass.: MIT Press, (2008).
19. S. Arlot, A. Celisse, *A survey of cross-validation procedures for model selection*, *Statist. Surv.*, **4** (2010).
20. P.I. Frazier, *A Tutorial on Bayesian Optimization*, (2018).

# DuEPublico

Duisburg-Essen Publications online

UNIVERSITÄT  
D U I S B U R G  
E S S E N

*Offen im Denken*

ub | universitäts  
bibliothek

This text is made available via DuEPublico, the institutional repository of the University of Duisburg-Essen. This version may eventually differ from another version distributed by a commercial publisher.

**DOI:** 10.17185/duepublico/83849

**URN:** urn:nbn:de:hbz:465-20250630-074701-5

First published in: SPE ANTEC® 2022 - Proceedings. SPE, 2022  
SPE ANTEC® 2024, Charlotte, NC, June 14-16, 2022.

© The authors. All rights reserved.